

An Approach for Evaluating Robustness of Edge Operators using Real-World Driving Scenes

Ali Al-Sarraf¹, Tobi Vaudrey¹, Reinhard Klette¹ and Young Woon Woo²

¹ The *.enpeda..* Project, The University of Auckland, New Zealand

² Department of Multimedia Engineering, Dong-Eui University, Busan, Korea

Abstract

Over the past 20 years there have been many papers that compare and evaluate different edge operators. Most of them focus on accuracy and also do comparisons against synthetic data. This paper focuses on real-world driver assistance scenes and does a comparison based on robustness. The three edge operators compared are Sobel, Canny and the under-publicized phase-based Kovese-Owens operator. The Kovese-Owens operator has the distinct advantage that it uses one pre-selected set of parameters and can work across almost any type of scene, where as other operators require parameter tuning. The results from our comparison show that the Kovese-Owens operator is the most robust of the three, and can get decent results, even under weak illumination and varying gradients in the images.

Keywords: edge operators, edge robustness evaluation, Kovese-Owens, phase operators

1 Introduction

Edge detectors play an important role in *driver assistance systems* (DAS). Optical flow algorithms typically only may derive correct results on edges. For dense flow algorithms (e.g., [6]), these results are smoothed over the image. Stereo algorithms (e.g., [9]) also get the best information for matching on edges. Robustly detecting edges will benefit both types of algorithms.

In the literature, there has been an ample amount of work performed on the performance of edge detectors, e.g. [17, 20, 22]. In this work many different performance measures are tested and used to compare different algorithms. [20] classified edge operators into the following types; gradient edge detectors (first derivative or classical), zero crossing (second derivative), Laplacian of Gaussian, Gaussian edge detectors and colored edge detectors. The edge detectors compared and contrasted in our paper are the Canny [7] and Sobel [21] operators (considered the two ‘most popular’ detectors in academia and industry), both gradient edge detectors, and the under-publicised Kovese-Owens [11, 16] operator; which is a Fourier phase-based operator, so does not fit into any of the classifications in [20]. [20] state that “none of the proposed operators are fully satisfactory in real world”. We aim to show that the Kovese-Owens operator is more robust to real-world noise, and

does not require parameter tuning as other operators do, so can be applied to real world images.

All of the edge detector performance papers were focusing on errors from either synthetic scenes, or from common computer vision images (e.g., Lena, Baboon, Hamburg taxi). In our paper, we compare real-world DAS images, and focus on the robustness of the algorithms. This is done both subjectively and numerically. Subjective analysis compares the algorithms quality on various DAS images. The numerical analysis compares results obtained on the original images to results obtained on the same images when artificial Gaussian noise is added. This is (the common way) to simulate increased noisy data. Abutaleb’s higher-order entropy binarisation algorithm [23] is used to assist the comparison between the three operators.

Section 2 introduces the basic concepts of our paper, including a summary of the edge detectors used. Section 3 covers which data we use for our evaluations and identifies the approach we used to evaluate robustness. In Section 4 we highlight the results from our experiments. The final section concludes the paper.

2 Basic Concept

This paper deals with aspects of edge operators on real-world driver assistance scenes. This section will cover the context and concepts used for performance evaluations.

2.1 Driver Assistance Systems

Over the past few years, DAS have become an important field in computer vision, and can be considered one of the most challenging tasks. The reason it is so challenging is that real-world image sequences, with real world noise and other problems such as bad weather and varying illuminations between cameras, need to obtain results (accurate with respect to traffic context) in real-time. Furthermore, the analysis is of a dynamic environment (independently moving objects and obstacles) and the fact that images are taken from a moving platform add to the complexity. Advanced techniques, with the use of one or more cameras over several time frames, have been introduced as a way to make this process more robust and to help prevent accidents from occurring (e.g., [8]). Some of these systems, that are already commercially available, are the Mercedes-Benz Distronic System and the Toyota Motor Corporation Advanced Parking Guidance System (APGS).

2.2 Edge Operators

Edge operators have been used in many fields of computer vision (e.g., object tracking [4], optical flow evaluations [6], stereo analysis [9], segmentation [19] and object recognition [5]). We selected three edge operators representing different concepts.

2.2.1 Kovesei-Owens Phase Congruency

The Kovesei-Owens operator is a phase-based operator, where an edge is detected if response reaches a maximal phase value in Fourier components of an image. Gradient-based methods on the other hand detect an edge when a discontinuity reaches its highest gradient value.

This operator depends on the *local energy model* which is based on theoretical mathematics as in [3, 16, 18]. Our implementation follows [11, 12]. The used phase congruency formula [16] is as follows:

$$C_1(p) = \frac{\sum_n A_n(p) \cos(\phi_n(p) - \bar{\phi}(p))}{\sum_n A_n(p)} \quad (1)$$

where p represents the pixel location in the image, $A_n(p)$ is the amplitude of the n^{th} cosine component of the local signal at position p , and $\phi(p)$ is the local phase component of the Fourier signal at position p . The value of $\bar{\phi}(p)$ that maximises $C_1(p)$ in Equation (1) is the *objective* of the function at p ; see [16] for more details.

However, according to [11] this “straight-forward” phase congruency does not provide a good localization and it is sensitive to noise. [11] proposes a modified formulation of phase congruency, which



Figure 1: *Construction-Site* sequence [1], image number 31. Top row: original and Kovesei-Owens edge image. Bottom row: Canny and Sobel edge images.

provides a more localized response and better noise compensation. The formulation is as follows:

$$C_2(p) = \frac{\sum_n W(p) [A_n \Delta\Phi(p) - T]}{\sum_n A_n(p) + \varepsilon} \quad (2)$$

where

$$\Delta\Phi(p) = \cos(\phi_n(p) - \bar{\phi}(p)) - |\sin(\phi_n(p) - \bar{\phi}(p))|$$

$W(p)$ is the weight factor for frequency spread, T is the estimated noise influence, the $[\cdot]$ operator sets the value to zero if it is negative, and ε prevents numerical instability. $\Delta\Phi(p)$ represents the local signal energy, similar to the numerator in Equation (1). Again, the value of $\bar{\phi}(p)$ that maximises Equation (2) is the objective of the function; see [11] for more details.

The main benefit of this operator is that it can detect edges under different illumination conditions, for which gradient-based operators are sensitive, resulting in incorrect edge detection. According to [11], another problem for gradient-based operators is that they require modification of thresholds to detect edges over a number of images in a sequence. By using the phase congruency, a fixed threshold can be used and will provide edge detection over a number of images in a sequence. The implementation used for the evaluations in this paper is the Kovesei-Owens operator, provided by [14]. An example of the output of the Kovesei-Owens operator on our test data can be seen in Figure 1. A more conclusive study of phase-based methods can be found in [13].

2.2.2 Canny and Sobel operators

Canny [7] or Sobel [21] edge operators are known for a reasonable design strategy, or simplicity. We used the implementation provided by the OpenCV library [2]. Our Canny operator applies a low threshold of 50 and high threshold of 70. The Sobel operator uses the standard 3×3 kernel. An

example of the output of the both the Sobel and Canny operator on our test data can be seen in Figure 1.

3 Evaluation

The overall process is outlined in Figure 2; details are in the following subsections.

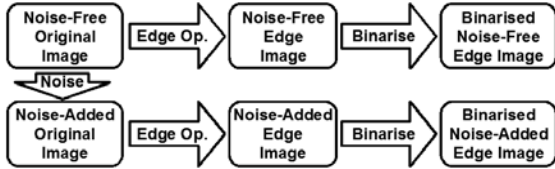


Figure 2: Overall process for evaluation.

3.1 Test Data

The test data, used in our evaluation, is a set of seven real-world rectified stereo image sequences, captured using stereo cameras mounted inside a moving vehicle. The image sequences are provided by Daimler AG (Germany), as part of an ongoing academic collaboration with The University of Auckland’s *.enpeda..* project. Each sequence provides a different scenario, with varying lighting conditions, contrast and road conditions. The sequences feature pedestrians, cyclists and animals as well as vehicles on the road. A brief explanation of each sequence is given below; for a more detailed explanation see [15].

Constructions-Site sequence: driving along the German Autobahn beside a construction site (road works); the weather condition is quite clear and the contrast of the images are quite high (e.g., Figure 1).

Safe-Turn sequence: driving in a small town with light traffic; the weather is a dark and cloudy, but the images have high contrast (e.g., Figure 3).

Squirrel sequence: driving on a road in the country side; dark and cloudy weather and low contrast.

Dancing-Light sequence: driving on the country side passing through a lot of trees that generate a lot of shadows on the road and vehicles; the weather is very sunny, but the shadows cause varying contrasts between images in a sequence (e.g., Figure 5).

Intern-on-Bike sequence: driving in a test area with a cyclist almost hitting the ego-vehicle; weather is clear sky and images have high contrast.

Traffic-Light sequence: driving on a very narrow country road; weather is masked by the surrounding trees, but the images have high contrast.

Crazy-Turn sequence: driving toward a main road and then taking a risky left turn at an intersection; the weather condition is quite cloudy and images have low contrast.

These stereo image sequences can be downloaded from the website [1].

3.2 Addition of Noise

We applied Gaussian “salt and pepper” noise to the images with a sigma of 10. This introduction of noise to the images is to help assess the robustness of the algorithms under bad sampling conditions.

3.3 Subjective Evaluation

From our seven sequences we selected 3 different scenarios, the subjective criteria in each scenario is to detect the distant vehicles, road signs and lanes. The main difference between the sequences is the image contrast. Using this evaluation we can visually see how robust the three operators are on the original images. After this subjective test on the original images, the operators are tested on the noise-added images to note the effects.

3.4 Numerical Evaluation

For our numerical evaluation we generated binarised images of the Kovesei-Owens and Sobel images. The binarisation was performed using Abutaleb’s higher-order entropy binarisation algorithm [23]. The reason for generating binary images of the edge processed test data was to compare the results against Canny, which is implicitly a binary result.

We define a set $A \in \Omega$ (Ω is the image domain) by the points identified from the ground truth binarised edge image. Here, the ground truth image is the binarised edge image computed on the noise-free image (see Figure 2). Set $B \in \Omega$ are the points identified from the comparison binarised edge image. Here, the comparison image is the binarised noise-added edge image (see Figure 2). The metrics we calculate are the symmetric correctness C , symmetric false positives E^+ , and symmetric false negatives E^- . They are defined as follows:

$$\begin{aligned}
 C &= \frac{|A \cap B|}{|A \cup B|} \times 100\% \\
 E^+ &= \frac{(|B| - |A \cap B|)}{|A \cup B|} \times 100\% \\
 E^- &= \frac{(|A| - |A \cap B|)}{|A \cup B|} \times 100\%
 \end{aligned}$$

where $|\cdot|$ defines the cardinality of the set. These equations were derived from work in [10]. From the equations above, we can determine two signal to noise ratios (SNR); total SNR (SNR^T), and false positive SNR (SNR^+). They are defined as follows:

$$\begin{aligned}
 SNR^T &= C / (E^+ + E^-) \\
 SNR^+ &= C / E^+
 \end{aligned}$$

We believe that SNR^+ is a better metric for calculating the effect of noise, because false positives introduce new problems where as false negatives only reduce information. So this measure identifies which algorithm prevents new noise being added to the image.

4 Results

4.1 Noise-Free Subjective Evaluation

Construction-Site sequence. From the evaluation of this sequence, Image 31 can be seen in Figure 1. From these images it can be seen that the distant vehicles are detected clearly using the Kovesi-Owens and Canny operators. Sobel gives us an unclear layout of the vehicles. As for the road lanes, Kovesi-Owens and Canny gave a clear indication of the road lanes on both sides of the road. Sobel detects the road lanes, but not clearly.

Dancing-Light sequence. This sequence has a lot of problems with low contrast and shadows throughout the scene. An example of the evaluation was image number 48 (Figure 5). Under the shadows of the trees, Kovesi-Owens detects the moving ve-



Figure 3: *Safe-Turn* sequence, image number 33. Layout as Figure 1.

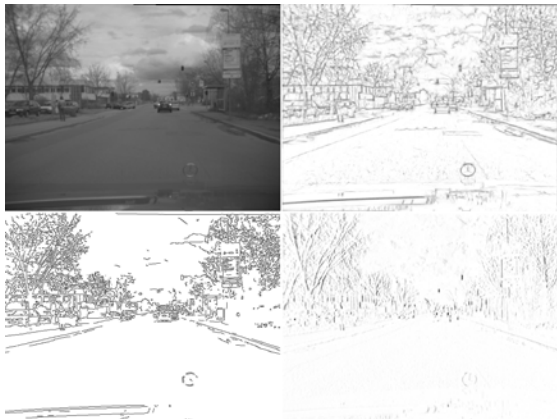


Figure 4: *Safe-Turn* sequence, image number 109. Layout as Figure 1.

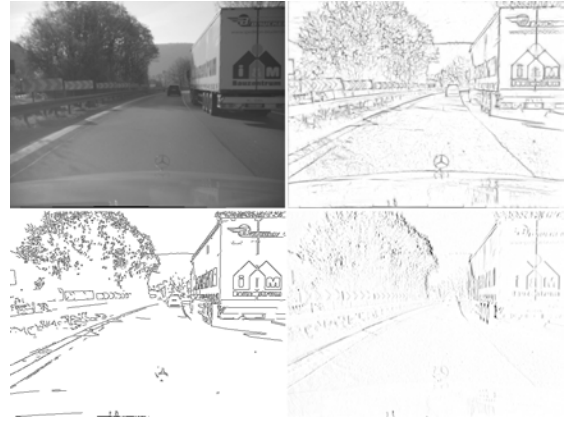


Figure 5: *Dancing-Light* sequence, image number 48. Layout as Figure 1.

hicle, road lanes and the road signs on the left. Canny detects the same but misses the road signs on the left. As for Sobel, it failed completely in detecting the distant vehicle and the road signs.

Safe-Turn sequence. In this scenario the images have a relatively high contrast. The example evaluations shown are image numbers 33 and 109. In image number 33 (Figure 3), Kovesi-Owens manages to detect the parking vehicle on the right, the distant vehicle, the three manholes and the road markings. Canny detects the parking vehicle completely, only two out of three manholes and half the right road lane. As for Sobel it was quite difficult to detect anything. The main points of interest here is the bottom left hand corner of the image and the right most manhole, where there is a very low contrast. Both Sobel and Canny are very weak and fail, but Kovesi-Owens still yields a strong edge detection.

As for image number 109 (Figure 4), all operators fail to give a clear indication that there is a pedestrian on the left hand side, but Kovesi-Owens detects the road bumps (middle of image) where Canny and Sobel fail.

4.2 Noise-Added Subjective Evaluation

In this section we give another subjective evaluation with Gaussian noise added to the original images. In all images you will notice that Canny is too full of noise to even be classed as providing meaningful results.

Construction-Site sequence. In all images (example image 179 shown in Figure 6), Kovesi-Owens gives a better result than the other two. It misses a few objects that were detectable on the original images (e.g. the road signs and lane), however the vehicles are still distinguishable.

Safe-Turn sequence. In example image 33 shown in Figure 7, Kovesi-Owens still detects the two manholes with good contrast, and other items on the

road. In the other two, all this information is lost under the noise.

Dancing-Light sequence. In example image 48 shown in Figure 8, Kovesi-Owens loses some detail on the



Figure 6: *Construction-Site* sequence image, number 179. Top row: noise added image and Kovesi-Owens edge image. Bottom row: Canny and Sobel edge images.

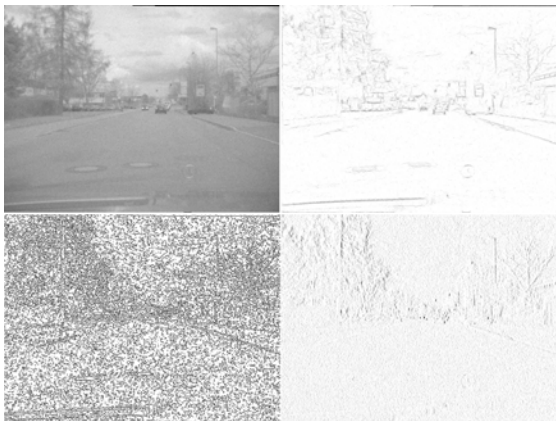


Figure 7: *Safe-Turn* sequence, image number 33: Top row: noise added image and Kovesi-Owens edge image. Bottom row: Canny and Sobel edge images.

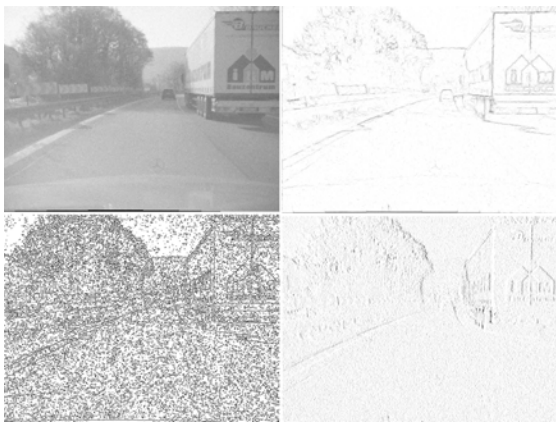


Figure 8: *Dancing-Light* sequence image, number 48. Top row: noise added image and Kovesi-Owens edge image. Bottom row: Canny and Sobel edge images.

signs, truck and road. However, the other two lose much more detail.

4.3 Numerical Evaluation

Examples of the binarised noise-free and the binarised noise-added edge images are in Figure 9.

The results in Table 1 show the results of our evaluation on the test data. It is clear that Canny is unreliable, with only 75% of the signal being correct. Sobel and Kovesi-Owens prove to be the most robust. On average, the Sobel operator detects the highest number of correct edges, but along with this is a large percentage of false positives. This is seen clearly by the lower SNR^+ . Sobel gives less false negatives than Kovesi-Owens. As seen by the higher SNR^T . However, we identified SNR^+ as the better evaluation for robustness, as for most follow-on processes a false positive is much worse than a false negative. For the SNR^+ , Kovesi-Owens outperforms Sobel by a large margin.

5 Conclusions

In this comparative study of edge operators on real-world driving scenes, we performed both subjective and numerical evaluations. We proposed a numerical method to evaluate robustness using real-world images.

From our evaluations, we conclude that the under-

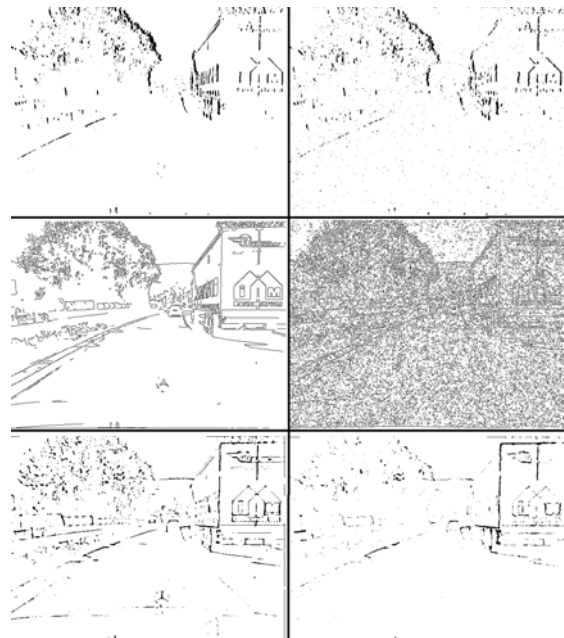


Figure 9: This figure shows an example (*Dancing-Light* image 48) of the binarised edge images used for numerical evaluation. Rows: Sobel (top), Canny (middle), Kovesi-Owens (bottom). Columns: Binarised noise-free edge image (left) and binarised noise-added edge image (right).

Seq.	Img. #	% Correct (C)			% False Neg. (E^-)			% False Pos. (E^+)			Total SNR^T			False Pos. SNR^+		
		Can.	K-O	Sob.	Can.	K-O	Sob.	Can.	K-O	Sob.	Can.	K-O	Sob.	Can.	K-O	Sob.
<i>Const. Site</i>	31 179	9 16	15 40	2 52	23 12	64 52	58 27	68 72	21 8	40 21	0.10 0.20	0.18 0.67	0.02 1.07	0.17 0.23	0.74 4.94	0.05 2.48
<i>Safe Turn</i>	33 109	14 21	41 12	49 52	13 17	37 55	17 24	73 62	22 33	33 24	0.17 0.27	0.700 0.14	0.97 1.07	0.20 0.34	1.90 0.38	1.48 2.15
<i>Danc. Light</i>	48	14	29	42	13	64	34	72	7	24	0.17	0.41	0.73	0.20	4.42	1.79
ALL	-	15	32	42	13	53	28	72	15	30	0.18	0.51	0.81	0.22	2.61	1.88

Table 1: A comparison of the Canny (Can.), Kovesei-Owens (K-O), and Sobel (Sob.) operators. The table highlights the images presented in this paper. The final summary (ALL) is the average result for every image in each sequence from Section 3.1. The metrics used are detailed in Section 3.4.

publicized Kovesei-Owens operator is the most robust of the three operators. Canny works well on noise-free images, but as soon as noise is introduced, this operator becomes unusable. Sobel performs well on both the noise-free and noisy images, but there are more apparent artifacts in the noise-added images compared to the Kovesei-Owens images. This is high-lighted with Sobel’s high E^+ .

In the subjective and numerical evaluation with the noisy images, Kovesei-Owens did not give us a higher percentage of detected edges, but it had a low SNR^+ . In the subjective section Kovesei-Owens still manages to give a good indication of the distant vehicles and some of the road lanes, compared to Canny and Sobel where they both failed to show proper results. The other major benefit of Kovesei-Owens is that it runs with fixed parameters and does not require tuning. We have confirmed that Kovesei-Owens is more robust than Canny and Sobel, even under different illuminations and weak image gradients.

References

- [1] .*enpeda.* Image Sequence Analysis Test Site. <http://www.mi.auckland.ac.nz/EISATS/>.
- [2] *Intel Reference Manual*, Open Source Computer Vision Library, <http://developer.intel.com>, 2001.
- [3] Y. Aw, R. Owens and J. Ross. An analysis of local energy and phase congruency models in visual feature detection, *J. Australian Math. Society*, Series B, Issue 40/1, pages 97–122, 1998.
- [4] M. Betke, E. Haritaoglu, and L. Davis. Multiple vehicle detection and tracking in hard real-time, in Proc. *IEEE Intelligent Vehicles Symposium*, pages. 351–356, 1996.
- [5] M. Betke and N. Makris. Information-conserving object recognition, in Proc. *Int. Conf. Computer Vision*, pages 145–152, 1998.
- [6] T. Brox, A. Bruhn, N. Papenberg, and J. Weickert. High accuracy optical flow estimation based on a theory for warping, In Proc. *ECCV*, pages 25–36, 2004.
- [7] J. Canny. A computational approach to edge detection, *IEEE Trans. Pattern Anal. Mach. Intell.*, 8:679–698, 1986.
- [8] U. Franke, C. Rabe, H. Badino, and S. Gehrig. 6d-vision: Fusion of stereo and motion for robust environment perception, in Proc. *Pattern Recognition (DAGM)*, pages 216–223, 2005.
- [9] S. Guan and R. Klette. Belief-propagation on edge images for stereo analysis of image sequences, in Proc. *Robot Vision*, pages 291–302, 2008.
- [10] R. Klette and P. Zamperoni. Measures of correspondence between binary patterns. *Image Vision Computing*, 5:287–295, 1987.
- [11] P. D. Kovesei. Image features from phase congruency, *J. Computer Vision Research*, 1:1–26, 1999.
- [12] P. D. Kovesei. Phase congruency detects corners and edges, in Proc. *DICTA*, pages 309–318, 2003.
- [13] P. D. Kovesei. Phase is an important low-level image invariant, *Advances in Image and Video Technology*, page 4, 2007.
- [14] P. D. Kovesei. Matlab and octave functions for computer vision and image processing, School of Computer Science & Software Engineering, The University of Western Australia, available from: <http://www.csse.uwa.edu.au/~pk/research/matlabfn/>.
- [15] Z. Liu and R. Klette. Performance evaluation of stereo and motion analysis on rectified image sequences, CITR, University of Auckland, Tech. Rep., 2007.
- [16] M. Morrone and R. Owens. Feature detection from local energy, *Pattern Recognition Letters*, 6:303–313, 1987.
- [17] T. B. Nguyen and D. Ziou, Contextual and non-contextual performance evaluation of edge detectors, *Pattern Recognition Letters*, 21:805–816, 2000.
- [18] B. Robbins and R. Owens. 2D Feature Detection via Local Energy, *Image and Vision Computing*, 15:353–368, 1997.
- [19] M. Rousson and R. Deriche. A variational framework for active and adaptive segmentation of vector valued images, in Proc. *Workshop on Motion and Video Computing*, pages 56–61, 2002.
- [20] M. Sharifi, M. Fathy and M.T. Mahmoudi. A classified and comparative study of edge detection algorithms, in Proc. *Information Technology: Coding and Computing*, pages 117–120, 2002.
- [21] I. Sobel and G. Feldman. A 3x3 isotropic gradient operator for image processing, talk presented at the Stanford Artificial Project in 1968.
- [22] L. Spreeuwers and F. van der Heijden. Evaluation of edge detectors using average risk, in Proc. *Pattern Recognition*, vol. 3, pages. 771–774, 1992.
- [23] Y.W. Woo, Performance evaluation of binarizations of scanned insect footprints, In Proc. *Combinatorial Image Analysis*, pages 669–678, 2005.